J Membrane Biol (2015) 248:1167–1173
DOI 10.1007/s00232-015-9834-5

The Roles of Tight Junctions and Claudin-1 in the Microbubble-Mediated Ultrasound-Induced Enhancement of Drug Concentrations in Rat Prostate

Yonggang Shang[1] · Xiaoxiao Dong[2] · Guangwei Han[3] · Jia Li[1] · Dong Cui[1] · Chengcheng Liu[4] · Longkun Li[1] · Shanhong Yi[1]

Received: 13 June 2015 / Accepted: 6 August 2015 / Published online: 20 August 2015
© Springer Science+Business Media New York 2015

Abstract Although microbubble-mediated ultrasound irradiation can enhance the prostate permeability, little is known about the mechanism. In our study, the healthy, adult male SD rats were divided into four groups: the BC, US, MB, and MMUS groups. A therapeutic ultrasound apparatus was used to treat the rats prostates in the presence of circulating MBs. Cefuroxime was injected to assess prostate permeability by HPLC. The structures of prostate tissues and TJs were observed by light and transmission electron microscopy. Western blot was used to assess claudin-1 expression. After treatment of microbubble-mediated ultrasound irradiation, the cefuroxime concentrations in the prostate were significantly increased. HE staining demonstrated that the gland epithelial cell layer became dropsical, thick, and disordered. In transmission electron microscopy, the TJs between adjacent capillary endothelial cells or gland epithelial cells were disjointed and partly interrupted. Furthermore, western blot showed the expression of claudin-1 was significantly decreased. However, these findings were not observed in the prostates exposed to microbubble or ultrasound alone, as well as the healthy control rats. In conclusion, microbubble-mediated ultrasound irradiation significantly enhanced the prostate permeability and improve the cefuroxime concentrations in prostate. The changes in TJs structure and the decreased claudin-1 expression may play important roles in this process.

Keywords Chronic prostatitis · Tight junctions · Claudin-1 · Microbubble · Ultrasound

Introduction

Chronic prostatitis (CP) is a common prostate disease (Shang et al. 2014a, b), about 30–40 % of young men suffer from this disease, and the incidence is increasing (Wallner et al. 2009). Patients with CP may be afflicted by irritative urinary symptoms, vague pelvic, or lower back discomfort and pain during or following ejaculation (Battikhi et al. 2006), and most of these are accompanied by anxiety, depression, and other psychiatric symptoms (Chung et al. 2011). CP seriously influences the patients' physical and mental health. In recent years, many studies have shown that CP is related to male infertility by reducing the semen quality of patients (Fu et al. 2014), and it is closely associated with the development of benign prostatic hyperplasia (Kramer et al. 2007) and prostate cancer (Nakai and Nonomura 2013). Therefore, it is needed to be prevented and treated.

Although a variety of methods are used to treat CP, the optimal treatment is still unknown and CP easily relapses in clinic (Shang et al. 2014a, b). Studies have shown that the main problem to cure CP is that many drugs are not able to fully infiltrate into the prostate tissue (Liu et al. 2010). Because of the composition structure of the prostate, scholars put forward the concept of "blood-prostate barrier" (Fulmer

✉ Shanhong Yi
yshh8810@126.com

[1] Department of Urology, Xinqiao Hospital, Third Military Medical University, Chongqing 400037, China

[2] Department of Ultrasound, Xinqiao Hospital, Third Military Medical University, Chongqing 400037, China

[3] Department of Urology, The 169th Hospital of People's Liberation Army, Hengyang 421002, Hunan Province, China

[4] Department of Urology, Chongqing Emergency Medical Center, Chongqing 400014, China

and Turner 2000), which is similar to the blood–brain barrier, and limits drugs enter the prostate gland. Hence, how to open this barrier and improve the permeability of prostate is a difficult and hot point. Contrast agent, microbubble-mediated ultrasound can increase the gaps between capillary endothelial cells and biological membranes by cavitation, which helps drugs permeation from plasma overflow vessels, and through biological membranes to reach the treatment sites (Shang et al. 2011). Previous study has showed that MB-mediated ultrasound irradiation can significantly improve the prostate permeability (Liu et al. 2013). However, the mechanism of this process is unclear, and it needs to be further studied.

In multicellular organisms, tight junctions (TJs) are one form of intercellular connections (Sawada et al. 2003), they are important in epithelial cell structures and biological functions and are the key link of the regulation of paracellular pathway permeability (Sawada 2013). TJs widely exist in the blood–brain barrier and blood–testis barrier (Cioni et al. 2012; Meng et al. 2005); and their regulation of permeability barrier has been a subject of attention of scholars in various fields. Claudins are the major transmembrane components of TJs. Studies demonstrated that claudins played important roles in the regulation of the blood–tumor barrier by MB-mediated ultrasound irradiation (Shang et al. 2011). In prostate, there are wide expressions of claudin-1, -3, -4, -5, -8, -7, -10 (Sakai et al. 2007), but whether TJs and claudins are involved in the regulation of prostate permeability by MB-mediated ultrasound irradiation is unclear. Hence, in this study, we planed to elaborate the roles of TJs and TJs-related protein claudin-1 in the MB-mediated ultrasound-induced enhancement of prostate permeability.

Materials and Methods

Animal Preparation and Group

The healthy, adult male Sprague-Dawley (SD) rats (about 200–300 g) were acquired from the Animal Center of Xiaoqiao Hospital, Third Military Medical University (Chongqing, China). Animals were randomly divided into four groups: the blank control group (BC group), ultrasound group (US group), MB group (MB group), and MB-mediated ultrasound group (MMUS group). The experimental protocols of all the rats were complied with the relevant ethical regulations.

Ultrasonic Therapeutic Apparatus and Microbubbles

The ultrasonic therapeutic apparatus and MBs were designed by the Department of Ultrasound, Xinqiao Hospital, Third Military Medical University. In the present study, the ultrasound parameters are as follows: frequency: 1.0 MHz; acoustic pressure: 500 kPa; acoustic intensity: 0.023 W/cm^2; duty ratio: 1.0 %; irradiation time: continuate 5 min. The MBs were lipid-coated with a mean particle diameter of 2 mm and a concentration of 9×10^{10}/mL. In a previous study, combined use of them enhanced the prostate permeability (Liu et al. 2013).

Experimental Treatments Exposure

In the MMUS group, rats were injected MBs (0.1 mL/kg) through caudal veins and prostates were insonated using the therapeutic apparatus; in the US group, prostates were insonated in the presence of a circulating saline injection (0.1 mL/kg); in the MB group, prostates received sham ultrasound exposure in the presence of circulating MBs (0.1 mL/kg) and in the BC group, prostates received sham ultrasound exposure in the presence of a circulating same dose of saline injection (0.1 mL/kg).

The Concentrations of Cefuroxime

Cefuroxime (CXM) injecta (0.75 g CXM dissolved in 80 mL saline) was used in 32 rats from the four groups ($n = 8$/group). All the rats were anesthetized and injected intravenously with CXM injecta (final dose 60 mg/kg) via tail veins after the respective treatments. 15 min after CMX injection, rats were killed by decapitation and prostates were acquired. Prostate tissue was rinsed with normal saline and dried with filter paper, weighed, and then prepared into tissue homogenate with 2 mL of normal saline and stored at −80 °C. The concentrations of CXM were measured with High-Performance Liquid Chromatography (Waters, America). The concentrations of eluted CXM were estimated from a standard curve ($y = 33066x - 2515.9$, $R^2 = 0.999$) generated through serial dilutions of CXM in distilled water. The permeability of prostate was assessed by eluted concentrations of CXM and expressed as micrograms of CXM per gram of dry prostate tissue.

Light and Transmission Electron Microscopy

20 rats from all groups ($n = 5$/group) were used for light and transmission electron microscopy analysis. After respective treatments, animals were killed and prostates were harvested. Half of the prostate tissue from each rat was incubated in 4 % paraformaldehyde for 24 h, then dehydrated in 85 % ethanol for 30 min, 95 % ethanol for 2 × 30 min, anhydrous ethanol for 3 × 30 min, acetone for 20 min, and xylene for 2 × 20 min. Prostate tissue was embedded in paraffins, and was cut into 4 μm tissue sections. These sections were stained using hematoxylin and eosin (HE) staining. And then sections were observed by light microscopy (Olympus BX50, Japan).

In electron microscopy, prostate was fixed with 2.5 % glutaraldehyde and successively dehydrated with 50, 70, 80, 90,100 % ethanol, then stained using 1 % methylene Blue-azure II stain. Super-thin sections were prepared and stained with uranyl acetate and lead citrate. Images were obtained under the transmission electron microscope (Philips Tecnai-10, USA).

Western Blot

After the respective treatments, 20 rats from all groups ($n = 5$/group) were killed and prostates were removed immediately. Prostate tissue was manually minced and subsequently homogenized in a glass homogenizer. Total proteins were extracted from prostate tissue using TriZol (Invitrogen, USA) and heated at 100 °C for 5 min. About 50 μg of protein were separated on a 15 % (v/v) SDS-PAGE gel. Then proteins were transferred onto PVDF membrane, and the membrane was probed with either mouse anti-claudin-1 (1:1000 dilution) from Abcam (Cambridge, USA) or mouse anti-GAPDH (1:1000 dilution) from Novus (USA) polyclonal antibodies for 24 h. After several washes, the membrane was incubated for 2 h with secondary goat anti-mouse IgG antibody conjugated with peroxidase (1:5000 dilution). The Roche chemiluminescence detection system (Roche, Basel, Switzerland) was used to visualize proteins of interest. The IDVs of protein bands were calculated by Quantity One Version 4.6.2 software (Bio-Rad, USA) and normalized with that of GAPDH.

Statistical Analysis

All data were expressed as the mean ± standard deviation (SD), and t test was used to determine the significant difference between two groups. One-way analysis of variance test was used to determine the significant difference among multiple groups. If the P value was <0.05, it was considered as statistically significant.

Results

The Concentrations of CXM in Prostate Tissue

As shown in Table 1, the concentrations of CXM in gram of dry prostate tissue in the BC, US, MB, and MMUS groups were (5.48 ± 4.19), (8.94 ± 11.26), (5.95 ± 3.74), and (16.58 ± 7.75)μg/mg, respectively. These results suggested that the concentrations of CXM in gram of dry prostate tissue were highest in the rats from the MMUS group; the difference between the MMUS and BC or US or MB group was significant ($P < 0.05$). However, no difference in CXM concentrations was found between the BC, US, and MB groups ($P > 0.05$).

Light and Transmission Electron Microscopy

The prostate tissues from the BC, US, and MB groups showed that the pseudostratified prostate gland epithelial cells retained arrangement, the cytoplasm and nucleus were uniform, and no other obvious abnormalities were observed by light microscopy (Fig. 1a, b, and c). However, HE staining of the prostate tissues from the MMUS group showed that the gland epithelial cell layer became dropsical and thick, the gland epithelial cells became swollen, and the arrangement of the glandular epithelial cell layer was disordered (Fig. 1d).

The transmission electron microscopy showed that the capillary endothelial cells of prostate tissues from the BC, MB, and US groups retained arrangement and close-knit, no obvious gaps between capillary endothelial cells were found, and the TJs were clearly visible (Fig. 2a, c, and e). The TJs between adjacent gland epithelial cells were tight and orderly (Fig. 2b, d, and f). However, in the MMUS group, capillary endothelial cells of prostate tissues were disorganized and widening cell gaps were found. The TJs between adjacent capillary endothelial cells or gland epithelial cells were disjointed and partly interrupted (Fig. 2g, h).

The Expression of Claudin-1

Western blot showed that TJ-related protein claudin-1 was expressed in all groups. The protein bands suggested that there was no difference in the expression of claudin-1 between the BC, US, and MB groups (Fig. 3a). However, the expression of claudin-1 was significantly decreased in the MMUS group (Fig. 3a). Figure 3b shows the the mean optical density values of claudin-1 using column chart.

Discussion

In our study, we found that the concentrations of CXM in prostate tissue were significantly increased, the TJs between adjacent capillary endothelial cells or gland

Table 1 The concentrations of CXM of dry prostate tissue (μg/mg)

Groups	BC group	US group	MB group	MMUS group
CXM concentrations	5.48 ± 4.19	8.94 ± 11.26	5.95 ± 3.74	16.58 ± 7.75*

* $P < 0.05$, MMUS group versus BC or US or MB group

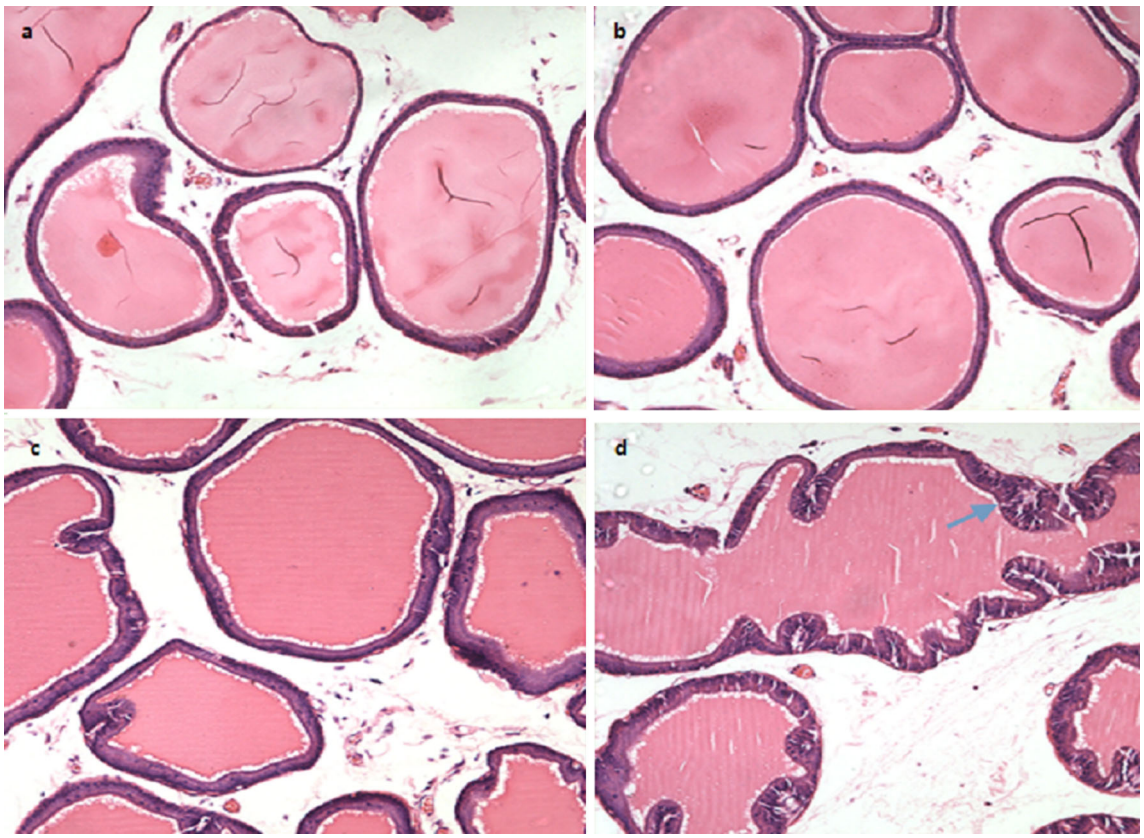

Fig. 1 HE staining of prostate tissues in different groups (×200). **a**, **b**, **c** The staining in the BC, US, and MB groups: no obvious disarrangement was found in the prostate gland epithelial cells layer, the cytoplasm and nucleus was uniform, and no other obvious abnormalities. **d** The staining in the MMUS group: clear edemata in the gland epithelial cell layer and swollen gland epithelial cells were found, the arrangement of the glandular epithelial cells was disordered (*blue arrow*) (Color figure online)

epithelial cells were disjointed and partly broken, and the expression of claudin-1 was significantly decreased after treatment of MB-mediated ultrasound irradiation. These results demonstrated that MB-mediated ultrasound irradiation enhanced the prostate permeability by opening TJs, and TJ-related protein claudin-1 may play an important role in this process.

Although MBs are a new ultrasound contrast agent which improves ultrasound imaging, they also mediate ultrasound-irradiation-enhanced tissue permeability and further make the drugs reach higher levels in the local tissues (Unger et al. 2001). Studies of the central nervous system diseases showed that MB-mediated ultrasound irradiation improved the permeability of blood–brain barrier (Huang et al. 2012; McDannold et al. 2011). In 2010, Liu et al. found that the concentrations of EB in prostate were increased after MB-mediated ultrasound irradiation; this result indicated that MB-mediated ultrasound irradiation could enhance the prostate permeability (Liu et al. 2010). In our study, we further observed that the concentrations of CXM, a commonly used drug for acute and CP, were significantly increased after treatment of MB-mediated ultrasound irradiation. Thus, this may be a new therapeutic method for CP. However, only few studies have focused on the mechanism of this process; therefore further studies are warranted to understand the mechanism.

Many studies considered that there was a structure between the blood and prostate glandular cavity, similar to the blood–brain barrier, and this structure plays an important role in the selective permeability of prostate, and protects prostate from damages (Motrich et al. 2006); however, it also restrains the drugs from entering the prostate when diseases occur (Charalabopoulos et al. 2003). Although this structure may be the major factor leading to the failure of treatment of CP, the main components are unclear (Shang et al. 2014a, b). The drugs from the blood to the prostate cavity mainly passes through capillary endothelial cells, fibrous tissue, basement membrane, and glandular epithelium cells (Wientjes et al. 2005); hence, one or more of these components are the main structure of regulating the permeability of the prostate. Regardless of the components of this barrier structure, the main structures which regulate the tissue permeability include the transcellular and paracellular pathways. Among

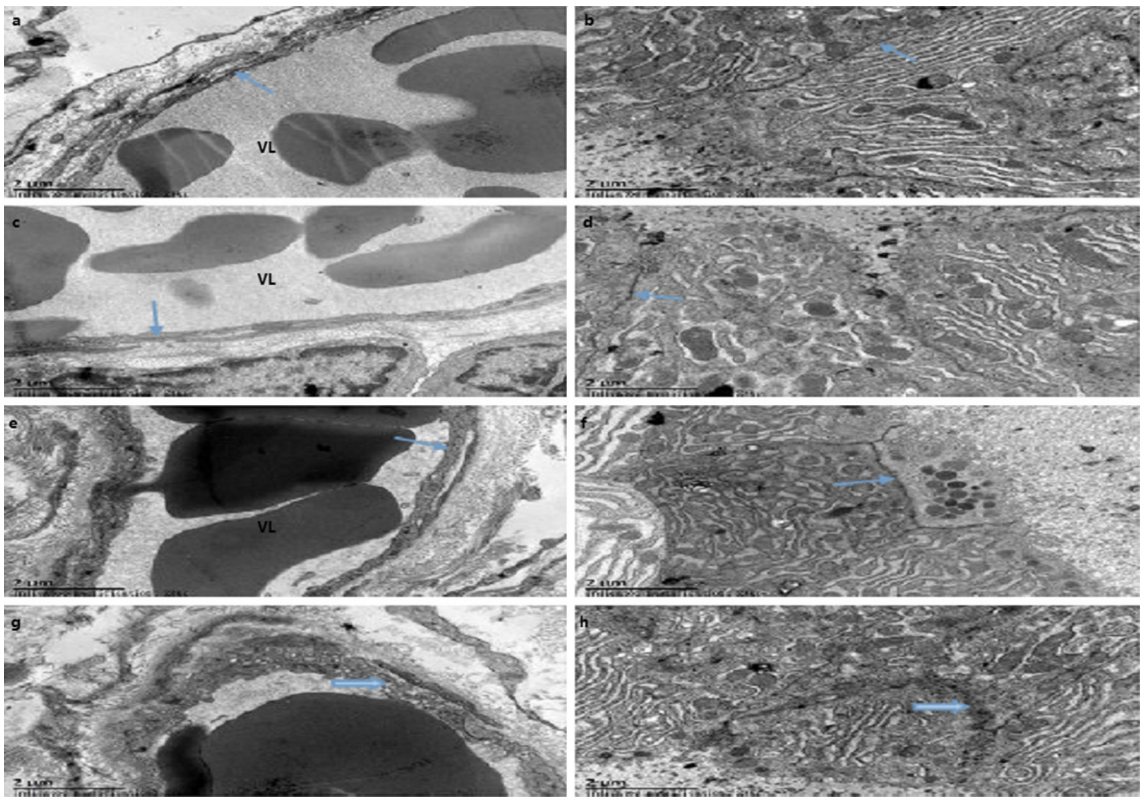

Fig. 2 Transmission electron microscopy of prostate tissues in each group (×20,000). **a** and **b** In the BC group: the capillary endothelial cells retained arrangement and close-knit (*thin blue arrow*), with no obvious gaps between the capillary endothelial cells or gland epithelial cells, and the TJs exist between cells (*thin blue arrow*). **c** and **d** In the US group: no disarrangement was found between the capillary endothelial cells (*thin blue arrow*), the TJs between adjacent capillary endothelial cells or gland epithelial cells were tight (*thin blue arrow*). **e** and **f** In the MB group: As same the BC and US groups, no obvious disarrangement was found and the TJs exist between adjacent cells (*thin blue arrow*). **g** and **h** In the MMUS group, obvious disarrangement and widening gaps in the capillary endothelial cell layer were found (*thick blue arrow*). The TJs between adjacent cells were disjointed and partly interrupted (*thick blue arrow*) (Color figure online)

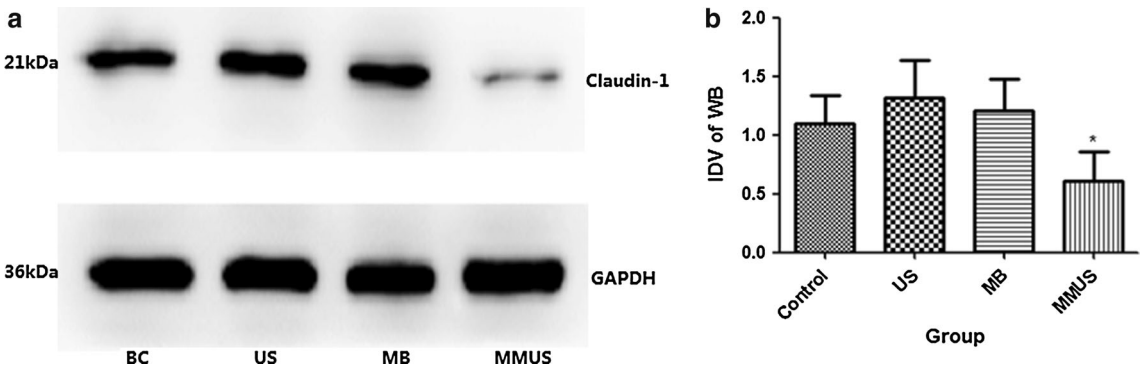

Fig. 3 Weston blot showed that expression of claudin-1 in each group. **a** Protein bands of claudin-1 expression in prostate tissue. The expression of claudin-1 were significantly decreased in the MMUS group, and there was no difference between the BC, US, and MB groups. **b** The IDVs in different groups. Values present mean ± SD (5 rats/group). *$P < 0.05$, MMUS versus BC, US, and MB groups

them, the TJs are the main functional areas of the regulation of the paracellular pathway permeability. Studies have shown that the intercellular permeability was significantly enhanced after opening the TJs in the blood–brain barrier (Beard et al. 2011; Chai et al. 2014). In the autoimmune prostatitis model, the inflammation can be inhibited after supplementing a certain amount of androgen, because the TJs are the key points for the androgen regulation (Meng

et al. 2011). Previously, Liu et al. showed that the concentrations of Evans blue (EB) in the prostate were increased after treatment of MB-mediated low frequency ultrasound irradiation, and over 24 h, EB concentrations were remarkably reduced, and transmission electron microscope observed the TJs were destroyed between adjacent cells but restored after 24 h (Liu et al. 2013). These findings suggested that TJs might be closely related to the prostate permeability. In the present study, we further showed that the TJs between adjacent capillary endothelial cells or gland epithelial cells were disjointed and partly broken after the prostate permeability being enhanced using MB-mediated ultrasound irradiation. These results suggest that TJs play an important role in the MB-mediated ultrasound-induced enhancement of prostate permeability.

TJs mainly consist of occludin, claudins, junctional adhesion molecule (JAM) and cytoplasmic attachment proteins (ZOs). Among them, occludin and claudins may play primary roles in regulating the TJs function and claudins are even more important (Oliveira and Morgado-Díaz 2007). Claudins are the essential components of TJs, and they widely present in the epithelia and endothelia. The protein kinase pathway-PKA or PKC acts on a specific amino acid target of claudins to regulate the selective permeability of the TJs, further changing the function of TJs (Fontijn et al. 2008). Claudin-1 belongs to one of the claudins family. A study showed that inducing the overexpression of claudin-1 could create a TJ structure in the fibroblasts (Furuse et al. 1998); this result suggested the importance of claudin-1 in the assembly of TJs. In brain, TJs are the critical structure in regulating the permeability of blood–brain barrier; the changes of claudin-1 expression are related to the regulation of BBB permeability (Sheehan et al. 2007; Neuhaus et al. 2008). Similarly, claudin-1 expresses both in the adjacent prostate capillary endothelial cells and gland epithelial cells (Sakai et al. 2007; Krajewska et al. 2007); however, whether it plays an important role in the regulation of prostate permeability is unclear, few studies have reported. In the present study, we found that the expression of claudin-1 in prostate was significantly reduced after the prostate permeability being enhanced by MB-mediated ultrasound irradiation. This suggests that claudin-1 is linked to the structure and function of TJs, and it plays an important role in the MB-mediated ultrasound-induced enhancement of prostate permeability.

Conclusions

The present study suggests that MB-mediated ultrasound irradiation can significantly enhance the prostate permeability and elevate the concentrations of CXM. The changes of TJs structure and the expression of TJ-related protein claudin-1 may play important roles in this process.

References

Battikhi MN, Ismail H, Battikhi Q (2006) Effects of chronic bacterial prostatitis on prostate specific antigen levels total and free in patients with benign prostatic hyperplasia and prostate cancer. Int Urol Nephrol 38:21–26

Beard RS Jr, Reynolds JJ, Bearden SE (2011) Hyperhomocysteinemia increases permeability of the blood-brain barrier by NMDA receptor-dependent regulation of adherens and tight junctions. Blood 118:2007–2014

Chai Q, He WQ, Zhou M, Lu H, Fu ZF (2014) Enhancement of blood-brain barrier permeability and reduction of tight junction protein expression are modulated by chemokines/cytokines induced by rabies virus infection. J Virol 88:4698–4710

Charalabopoulos K, Karachalios G, Baltogiannis D, Charalabopoulos A, Giannakopoulos X, Sofikitis N (2003) Penetration of antimicrobial agents into the prostate. Chemotherapy 49:269–279

Chung SD, Huang CC, Lin HC (2011) Chronic prostatitis and depressive disorder: a three year population-based study. J Affect Disord 134:404–409

Cioni C, Turlizzi E, Zanelli U, Oliveri G, Annunziata P (2012) Expression of tight junction and drug efflux transporter proteins in an in vitro model of human blood- brain barrier. Front Psychiatry 3:47

Fontijn RD, Volger OL, Fledderus JO, Reijerkerk A, de Vries HE, Horrevoets AJ (2008) SOX-18 controls endothelial-specific claudin-5 gene expression and barrier function. Am J Physiol Heart Circ Physiol 294:H891–H900

Fu W, Zhou Z, Liu S, Li Q, Yao J, Li W, Yan J (2014) The effect of chronic prostatitis/chronic pelvic pain syndrome (CP/CPPS) on semen parameters in human males: a systematic review and meta-analysis. PLoS One 9:e94991

Fulmer BR, Turner TT (2000) A blood-prostate barrier restricts cell and molecular movement across the rat ventral prostate epithelium. J Urol 163:1591–1594

Furuse M, Fujita K, Hiiragi T, Fujimoto K, Tsukita S (1998) Claudin-1 and -2: novel integral membrane proteins localizing at tight junctions with no sequence similarity to occludin. J Cell Biol 141:1539–1550

Huang Q, Deng J, Xie Z, Wang F, Chen S, Lei B, Liao P, Huang N, Wang Z, Wang Z, Cheng Y (2012) Effective gene transfer into central nervous system following ultrasound-microbubbles-induced opening of the blood-brain barrier. Ultrasound Med Biol 38:1234–1243

Krajewska M, Olson AH, Mercola D, Reed JC, Krajewski S (2007) Claudin-1 immuno-histochemistry for distinguishing malignant from benign epithelial lesions of prostate. Prostate 67:907–910

Kramer G, Mitteregger D, Marberger M (2007) Is benign prostatic hyperplasia (BPH) an immune inflammatory disease? Eur Urol 51:1202–1216

Liu Y, Liu Z, Li T, Ye G (2010) Ultrasonic sonoporation can enhance the prostate permeability. Med Hypotheses 74:449–451

Liu Y, Yi S, Zhang J, Fang Z, Zhou F, Jia W, Liu Z, Ye G (2013) Effect of microbubble-enhanced ultrasound on prostate permeability: a potential therapeutic method for prostate disease. Urology 81:921.e1–7

McDannold N, Zhang Y, Vykhodtseva N (2011) Blood-brain barrier disruption and vascular damage induced by ultrasound bursts combined with microbubbles can be influenced by choice of anesthesia protocol. Ultrasound Med Biol 37:1259–1270

Meng J, Holdcraft RW, Shima JE, Griswold MD, Braun RE (2005) Androgens regulate the permeability of the blood-testis barrier. Proc Natl Acad Sci USA 102:16696–16700

Meng J, Mostaghel EA, Vakar-Lopez F, Montgomery B, True L, Nelson PS (2011) Testosterone regulates tight junction proteins and influences prostatic autoimmune responses. Horm Cancer 2:145–156

Motrich RD, Maccioni M, Ponce AA, Gatti GA, Oberti JP, Rivero VE (2006) Pathogenic consequences in semen quality of an autoimmune response against the prostate gland: from animal models to human disease. J Immunol 177:957–967

Nakai Y, Nonomura N (2013) Inflammation and prostate carcinogenesis. Int J Urol 20:150–160

Neuhaus W, Wirth M, Plattner VE, Germann B, Gabor F, Noe CR (2008) Expression of Claudin-1, Claudin-3 and Claudin-5 in human blood-brain barrier mimicking cell line ECV304 is inducible by glioma-conditioned media. Neurosci Lett 446:59–64

Oliveira SS, Morgado-Díaz JA (2007) Claudins: multifunctional players in epithelial tight junctions and their role in cancer. Cell Mol Life Sci 64:17–28

Sakai N, Chiba H, Fujita H, Akashi Y, Osanai M, Kojima T, Sawada N (2007) Expression patterns of claudin family of tight-junction proteins in the mouse prostate. Histochem Cell Biol 127:457–462

Sawada N (2013) Tight junction-related human diseases. Pathol Int 63(1):1–12

Sawada N, Murata M, Kikuchi K, Osanai M, Tobioka H, Kojima T, Chiba H (2003) Tight junctions and human diseases. Med Mol Morph 36:147–156

Shang X, Wang P, Liu Y, Zhang Z, Xue Y (2011) Mechanism of low-frequency ultrasound in opening blood-tumor barrier by tight junction. J Mol Neurosci 43:364–369

Shang Y, Cui D, Yi S (2014a) Opening tight junctions may be key to opening the blood-prostate barrier. Med Sci Monit 20:2504–2507

Shang Y, Liu C, Cui D, Han G, Yi S (2014b) The effect of chronic bacterial prostatitis on semen quality in adult men: a meta-analysis of case-control studies. Sci Rep 4:7233

Sheehan GM, Kallakury BV, Sheehan CE, Fisher HA, Kaufman RP Jr, Ross JS (2007) Loss of claudins-1 and -7 and expression of claudins-3 and -4 correlate with prognostic variables in prostatic adenocarcinomas. Hum Pathol 38:564–569

Unger EC, Hersh E, Vannan M, Matsunaga TO, McCreery T (2001) Local drug and gene delivery through microbubble. Prog Cardiovasc Dis 44:45–54

Wallner LP, Clemens JQ, Sarma AV (2009) Prevalence of and risk factors for prostatitis in African American men: the Flint Men's Health Study. Prostate 69:24–32

Wientjes MG, Zheng JH, Hu L, Gan Y, Au JL (2005) Intraprostatic chemotherapy: distribution and transport mechanisms. Clin Cancer Res 11:4204–4211